European Rotorcraft Forum

40th European Rotorcraft Forum
September 2 - 5, Southampton, UK
Paper 084

Wind Turbine Wake Encounter by Light Aircraft

Yaxing Wang, Mark White and George N. Barakos

School of Engineering, University of Liverpool, L69 3GH, U.K.
Email: yxwang@liverpool.ac.uk

Stephen Wheeler, Peter Tormey and Panagiota Pantazopoulou

Civil Aviation Authority, U.K.

Abstract

The wake vortices generated by a wind turbine or a wind farm could interference with passing-by flying vehicles. A wind turbine wake study using engineering wake modelling, CFD, LIDAR field measurement and piloted flight simulation are carried out at University of Liverpool in cooperation with CAA, UK. A modified Kocurek wind turbine wake vortex model has been developed to simulate wind turbine wakes. It has been validated on the MEXICO wind turbine with the PIV wind tunnel measurements and the full CFD wake simulation results. This wake vortex model was applied to a WTN250 wind turbine, which has been installed near the East Midlands Airport, UK, where field measurements of wind turbine wake using LIDAR were carried out. The LIDAR measurement data were compared with the wake velocity fields generated by different wake modelling methods. The WTN250 wind turbine wake velocities generated by the Kocurek wake vortex model were integrated into an aircraft flight dynamic model to simulate a wind turbine wake encounter scenario, designed for a light aircraft approaching an airport, where a wind turbine was installed. The severity of the wind turbine wake encounter was investigated using piloted flight simulations. The simulation results suggest that the wake generated minor upsets on the aircraft and resulted a severity rating of B if only the disturbances caused by wake velocity deficits were taken into account.

1 INTRODUCTION

The wake vortices generated by a wind turbine or a wind farm have similar, but not identical, characteristics as aircraft wake vortices. They can also be hazardous to passing-by flying vehicles as in the case of aircraft wake encounters. Wind turbine wakes have their own structure, duration and decay [12, 15]. With increasing size of the modern large wind turbine rotors, the strength and influencing region of the wind turbine wakes increase, which might potentially generate risk to nearby flying aircraft. In the UK wind turbines are being proposed and built close to aerodromes, indicating an urgent need to assess the potential impact of wake turbulence on aircraft and in particular, to light aircraft and helicopters [3]. So understanding and prediction of wind turbine wake characteristics are vital to prevent flight accidents during wind turbine wake encounters.

Wind turbine wakes can be divided into near and far wake regions [12, 15]. The near wake is the area just behind the rotor approximately up to one rotor diameter downstream, where the effect of rotor properties, including the blade aerodynamics and geometry determine the flow field. The near wake research is focused on the wind turbine performance and the physics of power extraction. The far wake is the region beyond the near wake, where the details of the rotor are less important. The main interest in this area is the wake interference with other wind turbines (wind farm) or passing-by aircraft (wind turbine wake encounter). Here, the flow convection and turbulent diffusion are the two main mechanisms that determine the far flow field.

There are similarities between helicopter rotor wakes and wind turbine wakes and the vortex methods that are used for the analysis of helicopter wake problems can be adopted to represent the strengths and the spatial locations of the vortical wake elements that are trailed by each blade and convected into downstream. Prescribed vortex wake models [7] have also been developed for wind turbine applications. Like the helicopter rotor wake cases, the models are usually based on the assumption of incompressible, potential flow, and experimental observations.

CFD simulation of wind turbine wakes is an active area of research, and with increasing computer power, grid-based CFD simulation of wind turbine from Navier–Stokes (NS) equations are practical. However, the far wake simulation needs fine grid resolution. Actuator disk [12, 15] and actuator line [14] methods were used to simulate the rotor and the rest of flow was simulated by solving the NS equations, which enabled the CFD domain to cover the region extending from rotor plane to several diameters downstream to study both the near and far wake development. Recently full CFD methods [4, 5] were used to study the wake development and breakdown. These methods are very computationally expensive and require very fine grid to cover the far wake region. In most CFD wake studies, the flow conditions were treated

as ideal. The effects of wind shear, terrain and ambient turbulence were normally ignored. This results in predictions that show much stronger and coherent vortices.

Most of the wind turbine wake wind tunnel measurements in the published papers were focused on the near-wake due to technical challenges of the experimental setup. With the advance of LIDAR technology, field measurements are possible, in which the near and far wakes could be measured. LIDAR measurements results are still rare and not in the public domain. The LIDAR data are also highly dependent on the local atmospheric and environmental conditions. Since CFD simulations and different wake models need to be verified with experimental data, the aerodynamic research on wind energy shifts towards a more fundamental approach based on experiments in controlled conditions. In the USA, the NREL unsteady aerodynamic experiments of a full-scale rotor were conducted in the NASA-Ames 24.4m X 36.6m wind tunnel. The wind turbine is a two-bladed rotor with a diameter of 10m. In the NREL project, most of emphasis was put on pressure distribution measurements over the blade and hardly any wake measurements were conducted. In the Europe, a similar project called MEXICO (model rotor experiments under controlled conditions) was also conducted. A three-bladed rotor model of 4.5 m diameter was tested in the DNW (German-Dutch wind tunnel). In addition to pressure measurements on the blade surface, wake velocity measurements with PIV (particle image velocimetry) were also carried out.

A wind turbine wake study using engineering wake modelling, CFD, LIDAR field measurements and piloted fight simulations are carried out at University of Liverpool in cooperation with CAA, UK. The first results of this study are presented in this paper.

2 WIND TURBINE WAKE MODELLING

Modelling wind turbine wakes requires accurate prediction and simulation of wake vortex geometry, wake breakdown, mean velocity deficits and wake induced velocity flow-fields. There are several wake models available in the literature [12, 15] with different levels of complexity and fidelity. Three wake modelling methods are used in this study. These are the Kocurek wind turbine wake vortex model, the velocity deficit wake models and the full CFD method.

2.1 Kocurek wind turbine wake vortex model and validation

Wind turbine wake was firstly modelled using the modified Kocurek wind turbine wake vortex model [7] to capture the location and strength of the tip vortices. The Kocurek wind turbine wake vortex model was extended from the Kocurek-Tangler helicopter rotor hover wake model [8]. In the Kocurek-Tangler wake model, the wake vortex elements are positioned by prescribed functions which give axial settling and radial contraction rates in terms of basic inflow parameters. The tip vortex initially settles at a near constant rate until passing beneath the following blade, at which time the additional induced velocity from the second blade's bound vorticity and wake increase the settling rate. The radial contraction behaves exponentially with increasing wake azimuth, reaching a minimum wake radius. For the wind turbine case, due to the wind, the trajectory rates will be changed significantly by the axial transport. The wake transport is attributed to both induced velocities and wind. In the extreme case of very high wind speeds, there will be no much induced flow effect because of the high pitch or settling rate of the wake spiral. In normal working conditions, it is assumed that the wind speeds are sufficiently high to require only mean induced effects to be included in describing wake trajectories. In addition, wind turbine wakes expand rather than contract. Different flow states, which are determined by the axial velocity (corresponds to climb or descent rate for helicopter rotor) through the rotor are considered in this model to develop expressions for the axial and radial translation rates of the turbine wake. The normal state extends from hover through climb. From hover to decent, the rotor enters the vortex ring state in which the induced velocity is opposed to the descent speed. The streamline flow no longer exists and a highly unstable recirculating flow developed about the rotor. At further higher decent speeds, the rotor enters into the windmill brake state in which the streamline flow reorganises. This is the primary work state that wind turbines operate at. In the normal and windmill brake states, the disk momentum theory is applicable because of the existence of a continuous streamtube. In the vortex ring state, because of the breakdown of the streamline structure of the flow, the induced velocity only could be generated from empirical relationship.

For a wind turbine rotor disk, when the wake convects from upwind to downwind of rotor, the radial character of the wake changes from contraction to expansion. In order to determine the wake radius A and rate, the reference value of hover helicopter rotor A=0.78 is taken from the experimental measurements. The rate parameter is assumed to be inversely proportional to the wake pitch which sets the radial induced velocities.

The vortex circulation strength is dependent on the spanwise loading of the blade, the degree of the rolled-up of the tip vortex and changes induced by interference effects. The Beddoes circulation equation [2] was used to obtain the rolled-up tip vortex circulation.The initial tip vortex core radius was set to be 5 percent of the blade chord [2]. The formulae for wake vortex core growth [9] was used in the model to determine the core size.

The Kocurek wind turbine vortex model was applied to the MEXICO wind turbine, for which the PIV wind tunnel measurements of wake [13] and CFD simulation results [1, 4] are available for validation. The MEXICO wind turbine rotor was designed for an optimum tip speed ratio of 6.7, reached at a tunnel velocity of 15 m/s. The PIV measurements covered a region from approximately one diameter upstream to a little over one diameter downstream.

The tip vortices of the MEXICO wind turbine generated by the Kocurek wind turbine wake vortex model and the PIV measurements are shown in Fig. 1. The axial velocity contour plots were used to reveal the tip vortex structures in the wake. Compared with the PIV measurements, the individual vortex position in axial direction is accurately captured. The Kocurek model, however, over-predicts the radial position.

A full CFD study of the MEXICO wind turbine wake was also carried out at University of Liverpool [4] and the wake

vortices generated by the full CFD simulation were shown in Fig. 2. The flow field velocity comparisons of the Kocurek model and the full CFD simulation are presented in Fig. 3. Two values of thrust, one is CFD calculated and the other is experimentally measured, were used in the model to obtain the induced velocities. Both the axial (w) and the tangential (u) velocity components are shown good agreements. The fluctuations in the CFD velocity components are absent in the results of the Kocurek wake model due to its steady nature.

2.2 Wind turbine wake velocity deficit models

Wind turbine wake velocity deficit models are used in the wind energy industry to provide simple methods to study the wake interaction within a wind farm. These models are categorised into three families [12, 15]. The kinematic models are based on self-similar velocity deficit profiles and global momentum conservation. The wind turbine rotor thrust coefficient is the input. The wake growth is caused by ambient turbulence and the turbulence created by the shear in the wake. The field models use analytical forms of eddy viscosity to simulate turbulence and assume the wake flow is axial symmetrical. The boundary layer wake models consider the nonuniform atmospheric boundary layer and model turbulence transport by $k-\epsilon$ model. The Park and Katic [6] models, both of them are belong to kinematic model were used in this study to compare wind turbine wake velocity deficits with the LIDAR field measurements in the next section.

2.3 Wind turbine wake study by full CFD

At University of Liverpool, a full CFD method [4] was used in the HMB solver to study wind turbine wake. The CFD results showed good agreements of blade surface pressure distributions and flow field velocities to the wind tunnel measurements. The wake was then solved on a very fine mesh able to capture the wake vortices up to 8 radii downstream of the blades on the MEXICO wind turbine rotor. The location of the onset of instabilities and wake breakdown were predicted at wind speeds of 15 m/s and 10 m/s [5]. The CFD simulated wake vortices of the MEXICO wind turbine are shown in Fig. 2.

3 WIND TURBINE WAKE FIELD MEASUREMENT CAMPAIGN

A CAA-coordinated LIDAR measurement of wind turbine wake flow has been conducted in the East Mideast airport, where two WTN250 wind turbines (Fig.5) are installed and these are the first wind turbines that have been installed in the vicinity of an airport in UK. The WTN250 wind turbine has a 3-bladed up-wind rotor with a diameter of 30 m and a rotor speed 40 rpm.

The wind turbines were installed on the south side of the runway at a distance about 22.5 rotor diameters (675 m) from the runway. Due to the difficulty to obtain the planning permit from the wind turbine operator and manufacturer to install the LIDAR device on the nacelle in a short period of time, the LIDAR site (Fig. 6) had to be located on the northern slope of the runway, about 868 m from the wind turbines. where a nearby power station is available for supplying power to the LIDAR sensor system. The LIDAR set-up was carried out by SurrgEnergy engineers and the campaign started on 06/02/2014 and finished on 09/04/2014.

3.1 Galion LIDAR set-up and data processing

The Galion G4000 (Fig. 6) of SurrgEnergy was selected as the LIDAR to measure the wind turbine wake. The Galion is characterised as a second generation LIDAR device capable of varying the measurement beam in azimuth and/or elevation. It can provide an all sky scanning capability and up to 4 km range. The emitted laser beam is in the form of a pulsed laser with a frequency of 20 kHz. The distance is calculated from the time of flight of each range gate which in turn controls measurement points. The overlapping technique was adopted to refine the measurement resolution. Position Plane Indicator (PPI) scan or Arc scan (Fig. 7) was used in this campaign to measure the wind turbine wake flow. In PPI scan, multiple beams are used to build a detailed picture of the flow field over the designed region.

The azimuth range of the scan was set from 180.694^o to $186,454^o$ at an interval of 0.24^o. So the scan plane included 25 rays in azimuth. The scan covered an area from 478 m to 878 m in radial direction with a 3 m overlapping, which produced 133 measurement points per-ray. A single scan took 35 sec.

The LIDAR data was processed at each measurement point according to its azimuth and elevation angles. The flow velocity at each point was calculated from the Doppler signal which gave the line of sight velocity (the velocity along the ray).

Apparently, the current LIDAR set-up made the scan plane fixed in downwind region and could only capture the wind turbine wake flow fully when the wind was blowing from the south. It could also capture partially the wake if wind was blowing from south-east or south-west. Hence the scan data is only useful for these so-called ideal wind directions. The wind turbine cut-off wind speed is 4m/s which means that only when the wind speed is above 4m/s the scan data is meaningful for the wake measurements.

A wind screening processing is therefore required to pick up the meaningful scan data based on the wind data in freestream. The Meteorological Aerodrome Report (METAR) reports of EMA, which records the weather condition of the airport, are accessible on-line. The report can provide the half-an-hour averaged wind data in EMA. However, it is the overall wind data at the airport and is not very accurate for the measurement locations. The wind data measured by two on-site anemometers are also available. The location of one anemometer is close to the Galion LIDAR unit. It can provide the ten-minute statistic wind data to determine the wind conditions.

3.2 Results and discussion of the LIDAR campaign

Wind turbine wakes are characterised by reduced mean wind speeds (velocity deficit) and wake turbulence. In current LIDAR set-up, the measurements at each point were not simul-

taneous, so the LIDAR scan data can only capture the mean velocity deficits. Because the wind direction and speed constantly change with time, statistic measurement data are more appropriate to represent the averaged mean velocity deficits. In wind industry and weather forecast, ten-minute, half-hour and one-hour statistic data are widely used.

Typical LIDAR scan results of the WTN250 wind turbine wake are presented in Fig.8, Fig.9 and Fig.10, where ten-minutes averaged Line of Sight velocities from 14 pm to 15 pm on 07/04/2014 are plotted. The wind direction changes during this one-hour measurements were between 190 deg to 210 deg and the wind speed changes were between 17 kt to 18 kt. The one-hour averaged LIDAR data is shown in Fig. 11. The estimated location of wind turbine (the location was changed with wind direction as the rotor was turned into the incoming wind direction) as well as the arcs of one-diameter to five-diameter from the rotor hub were indicated in the figures. The one-hour statistic data reveal that the wake velocity deficit was recovered to approximately 10% of the free-stream wind speed at a downstream distance of 5D. Note that on the right side of the contour plots, there was a long low-speed contour bar that was extended to about to 2.5D in downwind. This was caused by the LIDAR laser striking on a solid or solids (most likely the blades, or the nacelle or the supporting tower) within the gate-range (30 m for current set-up). The velocity signals in this region were distorted without any physical meanings. This phenomenon is quite common in the LIDAR near wake measurements as can be seen in other datasets. The location of this distorted contour bar seems to be random. In some cases, there were more than one distorted contour bars in the wake velocity contour plots. Considerations must be taken in analysis of the measured data to to avoid any distractions by these near wake distortions.

In the figures, the wind turbine wake can be distinguished from the background free stream by the velocity deficit contours. The measurements indicated that statistically the mean velocity deficit was almost recovered to the free-stream wind speed in the downwind area about 5D from the rotor.

The LIDAR measurement was firstly compared with the full CFD results [5], indirectly, as the full CFD method was applied on the MEXICO rotor in an uniform inflow. At wind speed of 15 m/s, the MEXICO rotor tip speed ratio is 6.67. The full CFD results [5] revealed that wake vortices instability started at a position of about 2.5D downstream of the rotor and the breakdown occurred in downstream region from 3D to 4D. The mean velocity in the wake was about 9.5 m/s at the hub height (63% of the free stream wind speed) at 5D downstream. As a reference, at a wind speed of 10 m/s, the WTN250 wind turbine tip speed ratio is 6.3, close to that of the full CFD case.

The Park and Katic [6] wake velocity deficit models were applied to the WTN250 wind turbine at the wind speed of 10 m/s and the results are shown in Fig. 12. The park model and Katic model predicted the mean velocity deficit recovered to 10% of the free stream wind speed at about 4D and 8.5D, respectively. As in the full CFD case, in these models the effect of wind shear, terrain and ambient turbulence were not taken into account.

In general, the LIDAR measurements captured the regular wake mean velocity patterns. Statistic LIDAR data indicate that the effects wind turbine rotor wake, in term of velocity deficit, are limited within a downwind distance of 5D. This is generally in agreement with the results of the full CFD method and the velocity deficit models.

4 WIND TURBINE WAKE ENCOUNTER FLIGHT SIMULATION

The piloted wake encounter flight simulations were carried out in this study to investigate the severity of wind turbine wake encounter. The wake encountering aircraft is a GA training aircraft configured to be similar to a Grob Tutor light aircraft. During the simulation the rolling, pitching and yawing moments, aircraft altitude change, velocities and accelerations during an encounter were recorded together with the pilot's control inputs to capture a complete description of the encounter. This data provided a quantitative measure of the effect of the wake on the aircraft. After each set of runs the pilot was asked to rate the hazard using the Wake Vortex Severity Rating Scale [10].

4.1 Wake encounter scenarios

The wind turbine wake encounter scenario was designed for a light aircraft approaching an airport, where a WTN250 wind turbine was installed. the wind turbine wake might generate upsets on the passing-by aircraft. The WTN250 wind turbine rotor hub was positioned at a height of 100 ft above the ground and at several offsets from the centerline of the runway at orientation angles of 90^o and 45^o. The pilots were asked to fly the aircraft at different altitudes along the runway to penetrate the wind turbine wake to simulate the crossing and oblique wake encounters. A wind speed of 10 m/s was used in the simulation for the wake generation. In some simulation sorties, the pilots were asked to hold the controls during the encounter to measured the maximum attitude and altitude deviations without interventions of pilot. In each simulation sortie, the pilot was asked to give the subjective severity rating [10] if the wake was detected. The simulation scene is shown in Fig. 14 where the light aircraft is penetrating the wind turbine wake during approaching an airport.

4.2 Simulator, aircraft flight dynamics model and pilot rating scale

The simulator used in the trials is the HELIFLIGHT simulator [11]. It is a full motion simulator with a single-seat cockpit. There are 3 channels collimated visual displays for the Out-the-Window view and two chin-window displays. Pilot controls are provided by a four-axis dynamic control loading system. It has a six DOF full motion platform and the pilot is able to communicate with the control room at all times via a headset.

The aircraft flight dynamics model was developed in the FLIGHTLAB simulation package based on a Grob Tutor configuration. The main aircraft components of wing, fuselage, propeller, tail, fin, landing gears, engine and control system are modelled. The WTN250 wind turbine wake velocity fields generated by the Kocurek wind turbine wake vortex model

were integrated into the aircraft dynamics model as interference on the aircraft using look-up tables. The wake has an impact on the wings, fuselage, propellers, tail, fin and lift-surfaces.

During the trials, the pilot was asked to give feedback on the wake encounters and rate the severity according to a wake vortex encounter pilot rating scale, which is a scale that has been used in a previous study by Padfield et al [10]. It provides a simple decision tree that enables the pilot to provide a subjective assessment of the level of wake encounter hazard.

4.3 Simulation results and discussion

The results of a typical wake encounter are shown in Fig. 15, where the aircraft dynamic responses are plotted during the approach. In this case, the pilot flew the GA aircraft through the WTN250 wind turbine wake at a same altitude as the the height of the wind turbine rotor centre (100 ft) in the crossing encounter. The wake generated some upsets on the GA aircraft and a severity rating B was awarded by the pilot for this encounter. The results indicate that the wake mainly generated yaw disturbances on the aircraft and caused a yaw angle deviation which is no more than 10^o. Only minor control corrections were needed from pilots to rectify the flight path.

The most significant disturbance cased by a wind turbine wake is in its axial direction and manifested as a velocity deficit in the downwind region. Although the wake vortices also cause disturbances velocities in the radial and vertical direction, they are smaller than the axial disturbance velocity. The fluctuation of these velocities, which can be seen in the full CFD simulation (Fig. 3), were not captured in the current wind turbine wake model as the model is only for steady flow. So when the aircraft flew through the wind turbine wake, only these spatial axial velocity gradients had impacts on the aircraft's flight dynamics. The disturbances exerted side-forces on the aircraft and caused its yaw angle changes when it entered and left the wake region.

5 CONCLUSION AND FUTURE WORK

Different methods of modelling a wind turbine wake namely the Kocurek wind turbine wake vortex model, far-wake velocity deficit models and the full CFD method have been used to study wind turbine far wake. The Kocurek wake model has been validated with the wind tunnel experimental measurements on the MEXICO wind turbine. The wake induced velocities has been compared with the full CFD results. These comparisons prove that the Kocurek model predicts wind turbine wake with a reasonable accuracy.

The kocurek wind turbine vortex model was then applied on the WTN250 wind turbine, which was installed near the East Midland Airport, UK, and where a wind turbine wake field measurement using LIDAR was also carried out. The results of LIDAR measurements captured the wake flow patterns in terms of wake induced mean velocity deficit. The statistic LIDAR data indicated that for this particular wind turbine the wake mean velocities recovered to the free stream speed at a position about five rotor diameters downstream. The LIDAR measurements were compared with the results of a full CFD simulation, which was conducted on the MEXICO wind turbine with a similar tip speed ratio, and also compared with the velocity deficit wake models. In general, reasonable agreements were shown.

The WTN250 wake induced velocity fields, which was generated by the Kocurek wake vortex model, were integrated into an aircraft flight dynamic model based on a Grob tutor configuration to simulate the wind turbine wake encounter scenario of a light aircraft approaching an airport. Piloted flight simulations were carried out to study the severity of this type of wake encounter. The flight simulation results suggest that the WTN250 wind turbine wake mainly generated yaw disturbances on the encountering aircraft and caused a yaw angle deviation less than 10°. The wake encounter severity is regarded as minor.

It is recognised that either the Kocurek wake model or the current LIDAR measurements can only generate the wake velocity deficit flow fields. The mean velocity deficit in wind turbine wake normally decay faster than that of the wake turbulence. The wake turbulence might be persistent longer in downstream. If the length scales of the wake turbulence is compatible with the size of aircraft lifting surfaces, it could cause unsteady upsets on the encountering aircraft. So methods of modelling and measuring wind turbine wake turbulence will be sought and be implemented in the future wake encounter flight simulations. A helicopter model will be developed to simulate the wind turbine wake encounter in the same fashion. The responses of helicopter and pilots' controls are anticipated to be different due to the different flight dynamics.

Acknowledgements

The financial support from the Civil Aviation Authority (CAA) UK and the University of Liverpool is gratefully acknowledged. Thanks to SurrgEnergy for providing LIDAR and technical supports for the wind turbine field measurement campaign.

REFERENCES

[1] A. Becnmann, N.N. Sorensen, and F. Zahle. CFD simulations of the MEXICO rotor. *Wind Energy*, 14(5):677–689, 2011.

[2] T.S. Beddoes. A Wake Model for High Resolution Airloads. *U.S. Army/AHS Conference on Rotorcraft Basic Research*, February 1985.

[3] CAA. CAA Policy and Guidelines on Wind Turbines. Technical report, Civil Aviation Authority, January 2012.

[4] M. Carrion, R. Steijl, M. Woodgate, and G. Barakos. CFD Analysis of the Wake of the MEXICO Wind Turbine. *Wind Energy*, 00:1–17, 2012.

[5] M. Carrion, M. Woodgate, R. Steijl, G. Barakos, S. Gomez-Iradi, and X. Munduate. Understanding Wind Turbine Wake Breakdown Using CFD. *Journal of AIAA*, Accepted, 2014.

[6] I. Katic, J. Jojstrup, and N.O. Jensen. A Simple Model for Cluster Efficiency. *Proc. EWEC*, 1:407–410, 1986.

[7] D. Kocurek. Lifting Surface Performance Analysis for Horizontal Axis Wind Turbines. Technical Report SERI/STR-217-3163, Solar energy research institute, US department of energy, 1987.

[8] J.D. Kocurek and J.L. Tangler. A Prescribed Wake Lifting Surface Hover Performance Analysis. *Journal of the American Helicopter Society*, 22(1):24–35, January 1977.

[9] G. Leishman. *Principles of Helicopter Aerodynamics*. Cambridge aerospace series book, Cambridge, UK, second edition, 2007.

[10] G.D. Padfield, B. Manimala, and G.P. Turner. A Severity Analysis for Rotorcraft Encounters with Vortex Wakes. *Journal of American Helicopter Society*, 49(4):445–456, 2004.

[11] G.D. Padfield and M.D. White. Flight simulation in academia - heliflight in its first year of operation at the university of liverpool. *The Aeronautical Journal*, 107(1075):529–538, 2003.

[12] B. Sanderse. Aerodynamics of Wind Turbine Wakes. Technical Report ECN-E-09-016, Energy research centre of the Netherlands, 2000.

[13] H. Snel, J.G. Schepers, and B. Montgomerie. The MEXICO project: the database and first results of data processing and interpretation. *Journal of Physics: Conference Series*, 75(012014), 2007.

[14] N. Troldborg, J.N. Sorensen, and R. Mikkelsen. Numerical Simulations of Wake Characteristics of a Wind Turbine in Uniform Inflow. *Wind Energy*, 13:86–99, 2010.

[15] L. Vermeer, J. Sorensen, and A. Crespo. Wind Turbine Wake Aerodynamics. *Progress in Aerospace Sciences*, 39:467–510, 2003.

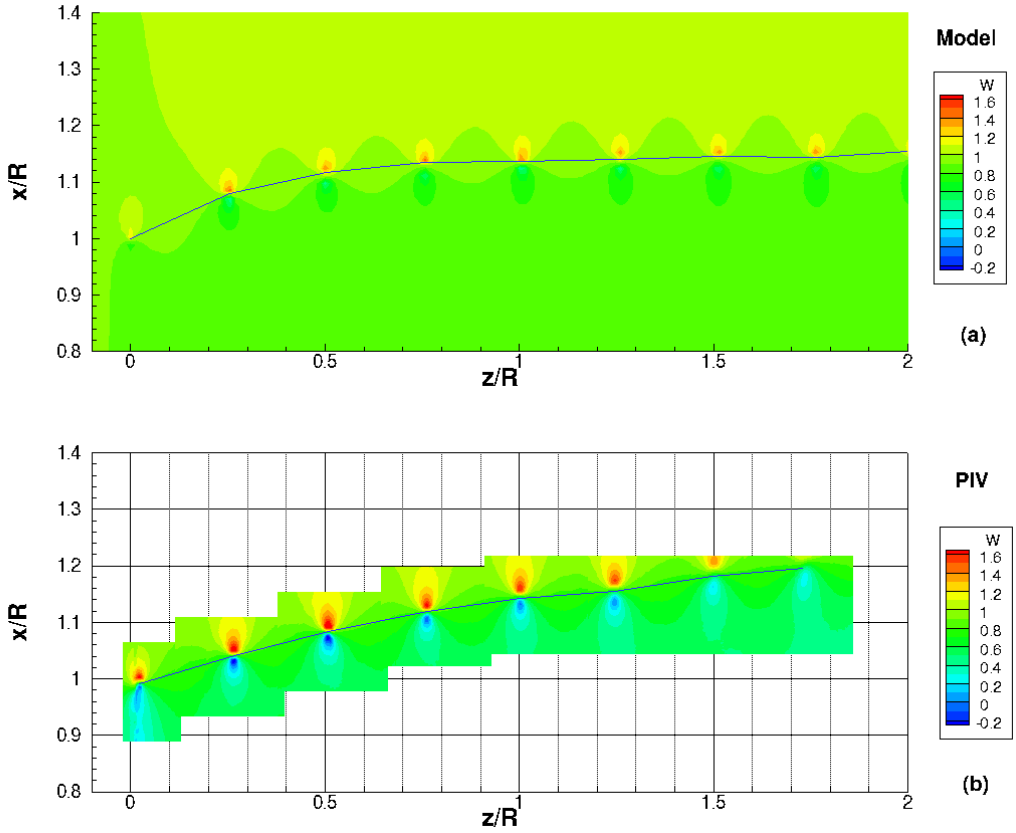

Figure 1: MEXICO wind turbine wake vortices at wind speed 15 m/s, (a) generated by the Kocurek wind turbine wake model, (b) PIV measurements.

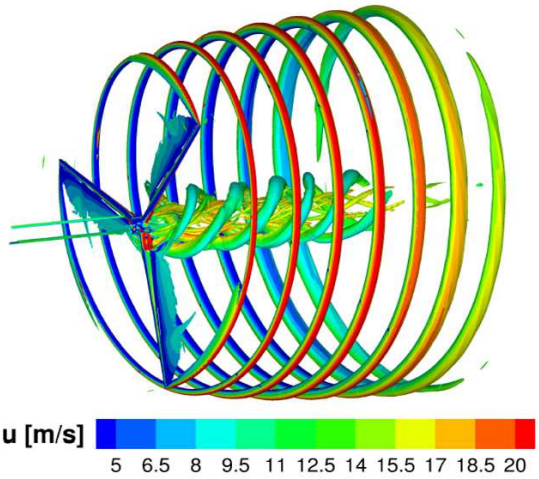

Figure 2: MEXICO wind turbine wake vortices generated by a full CFD simulation at wind speed 15 m/s [4].

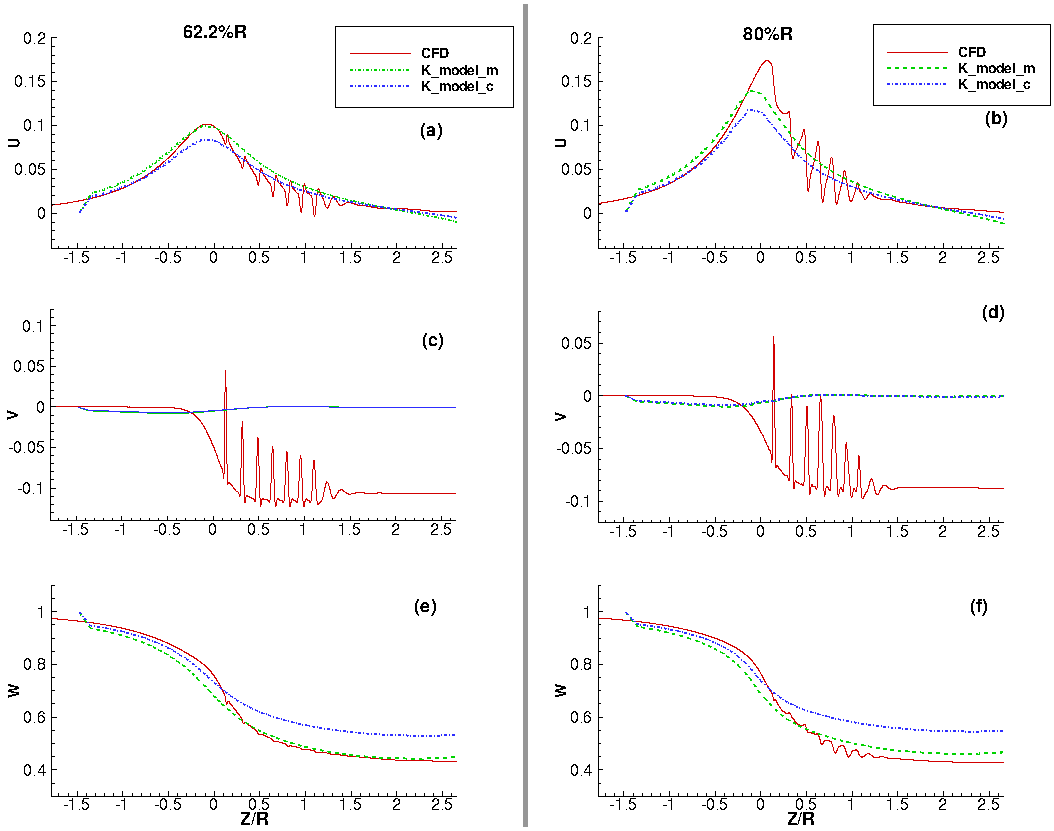

Figure 3: Comparisons of the tangential (u), radial (v) and axial (w) velocity profiles generated by Kocurek wake model and CFD [4] on the MEXICO wind turbine at 62.2%R (left column) and 80%R (right column), wind speed 15 m/s, the velocities were normalised by the wind speed. K_model_m: Kocurek wake model with the measured thrust; K_model_c: Kocurek wake model with the CFD calculated thrust.

Figure 4: WTN250 wind turbines of the East Midlands airport.

Figure 5: The WTN250 wind turbines and the runway of the East Midlands airport.

Figure 6: The Galion LIDAR on site.

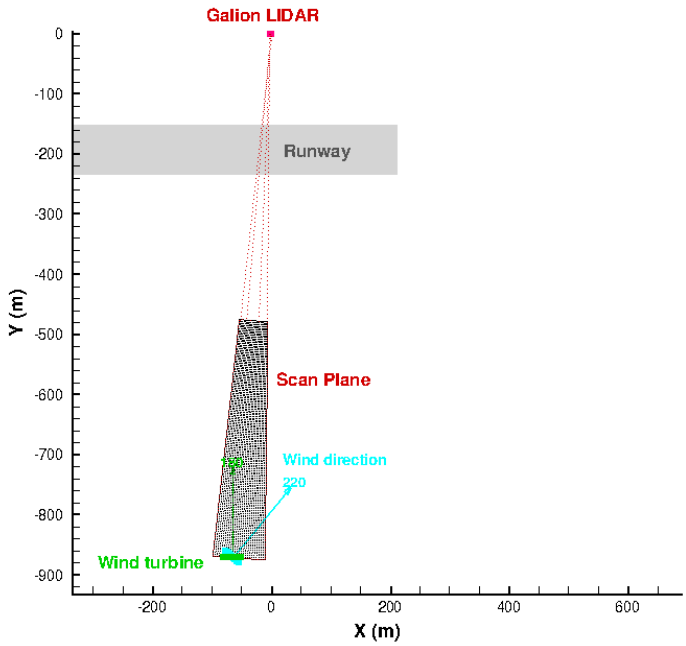

Figure 7: Schematic of the PPI scan plane for wind turbine wake measurements.

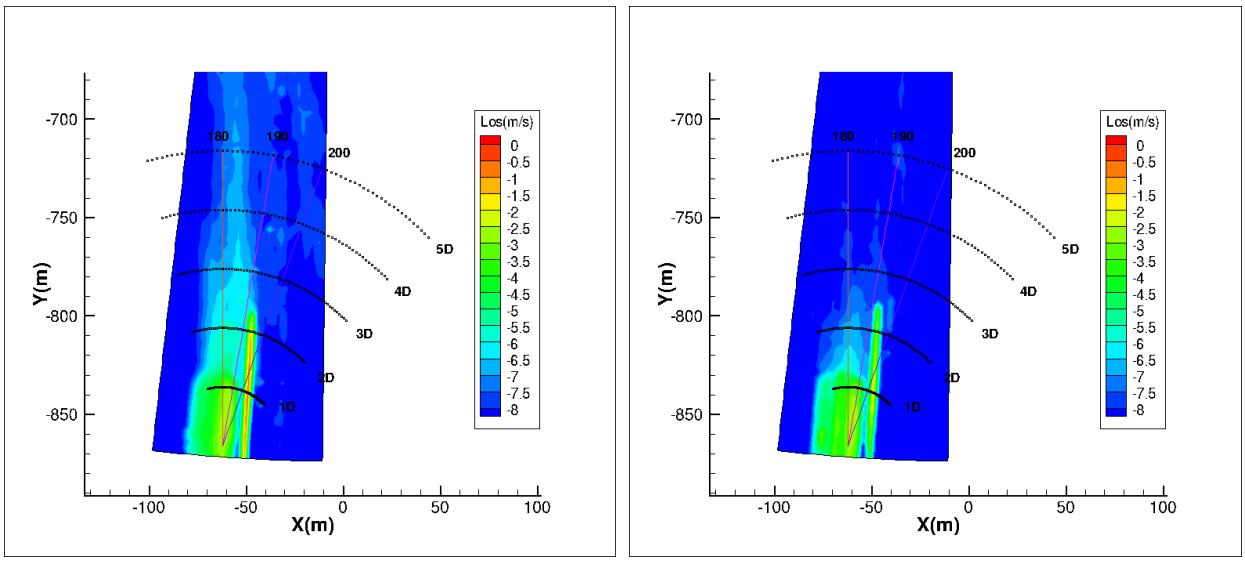

(a) From 14:00 to 14:10

(b) From 14:10 to 14:20

Figure 8: Ten-minute averaged line of sight velocity measured on 07-04-2014.

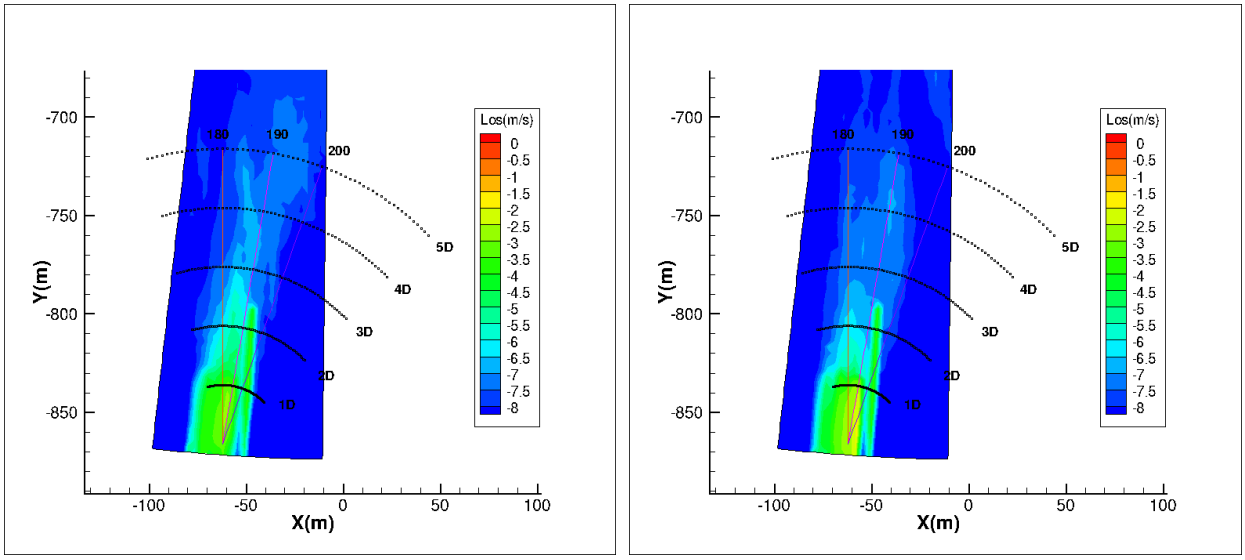

(a) From 14:20 to 14:30

(b) From 14:30 to 14:40

Figure 9: Ten-minute averaged line of sight velocity measured on 07-04-2014.

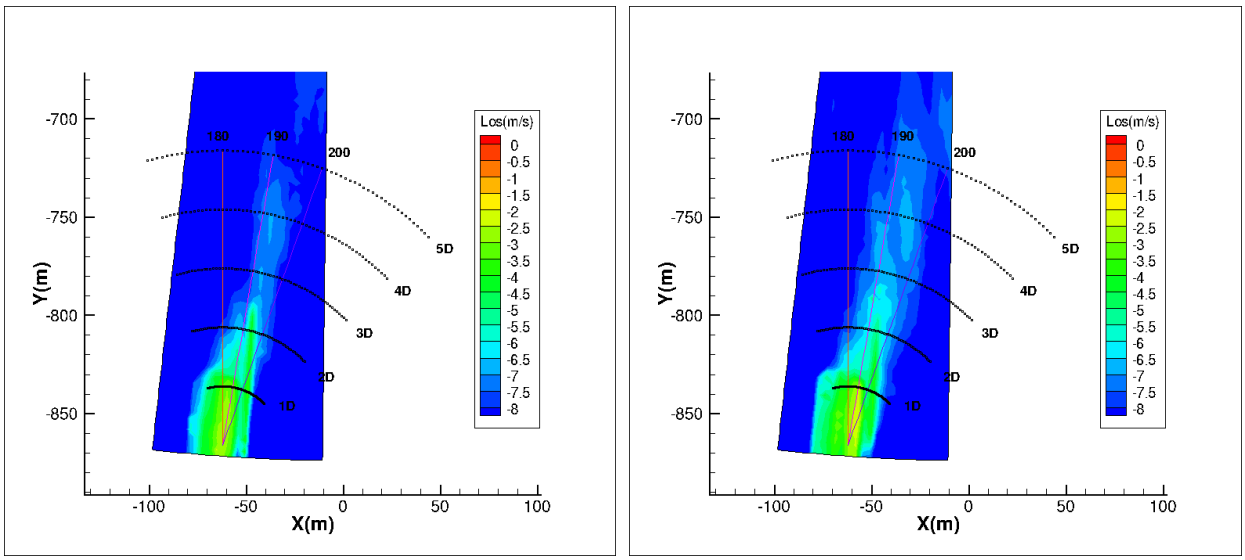

(a) From 14:40 to 14:50

(b) From 14:50 to 14:60

Figure 10: Ten-minute averaged line of sight velocity measured on 07-04-2014.

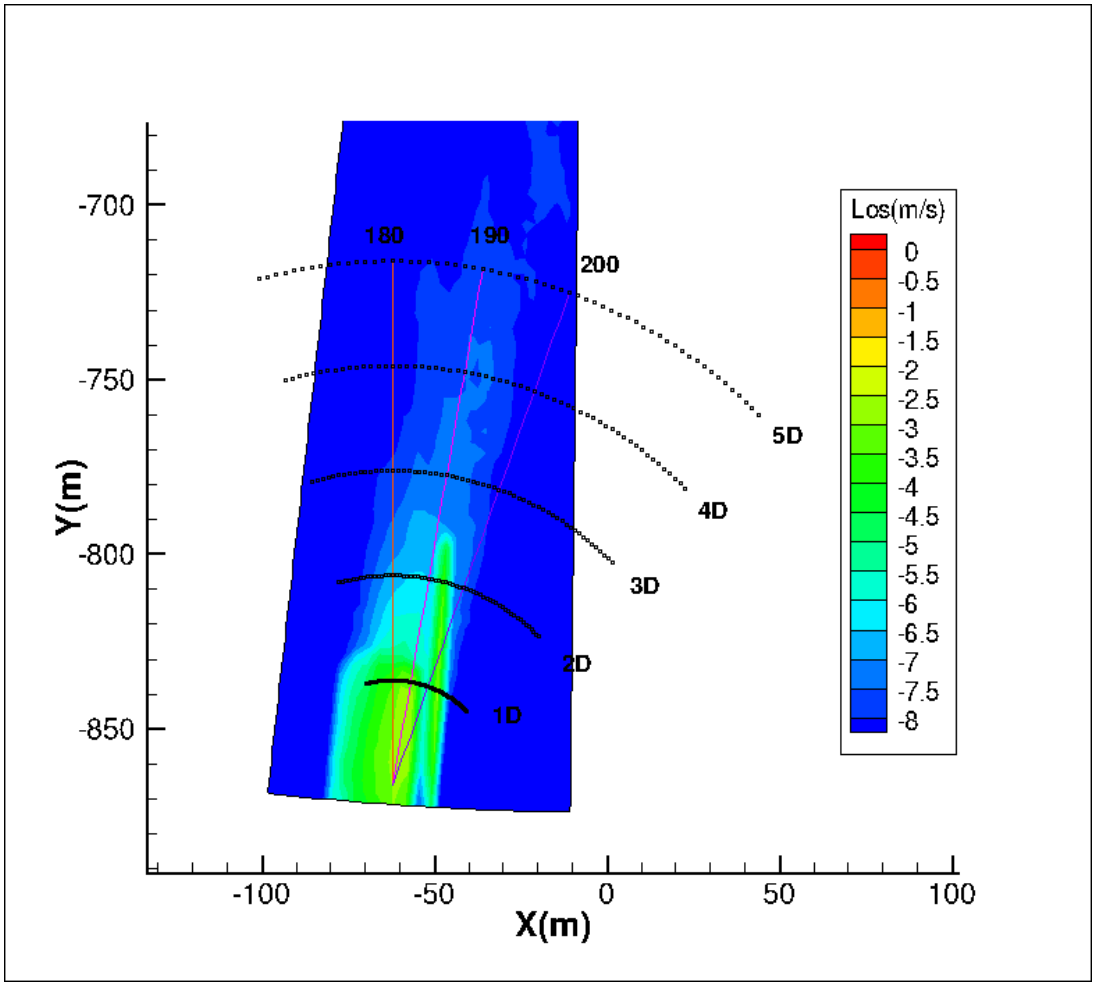

Figure 11: One-hour averaged line of sight velocity measured on 07-04-2014.

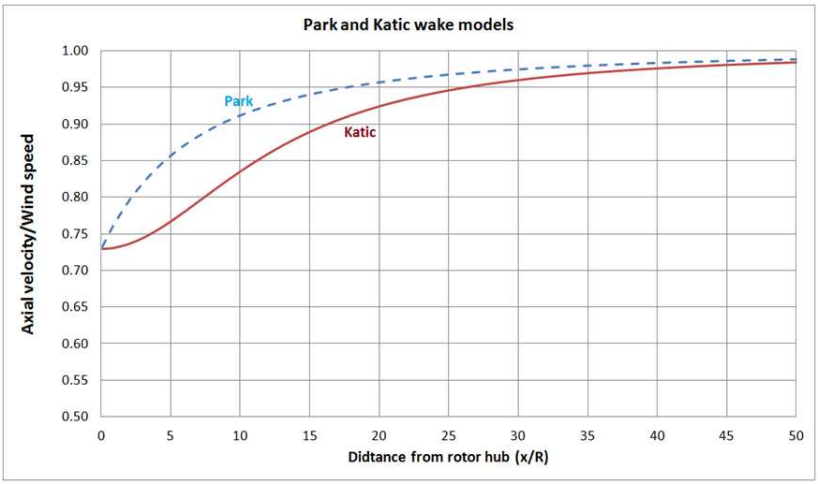

Figure 12: Wake velocity deficits using the Park and Katic models for an approximate WTN250 wind turbine at a wind speed of 10 m/s.

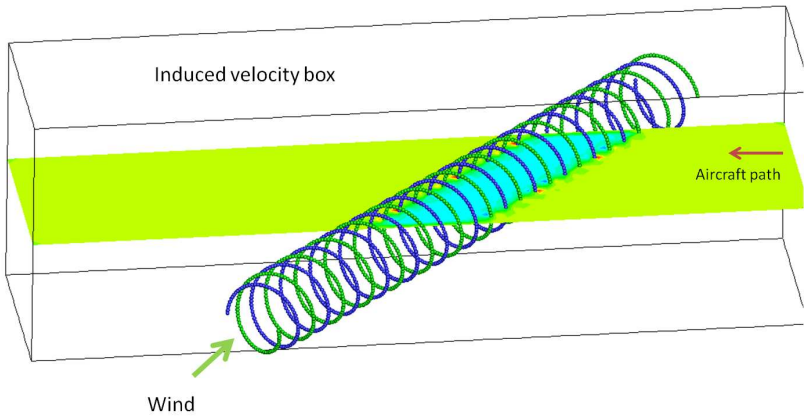

Figure 13: Oblique wind turbine (45^o) wake encounter scenario.

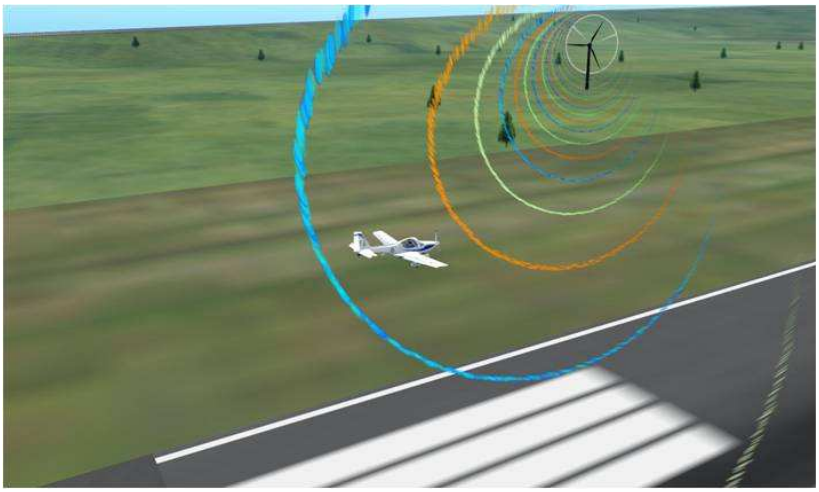

Figure 14: Simulation scene of a light aircraft encountering wind turbine wakes.

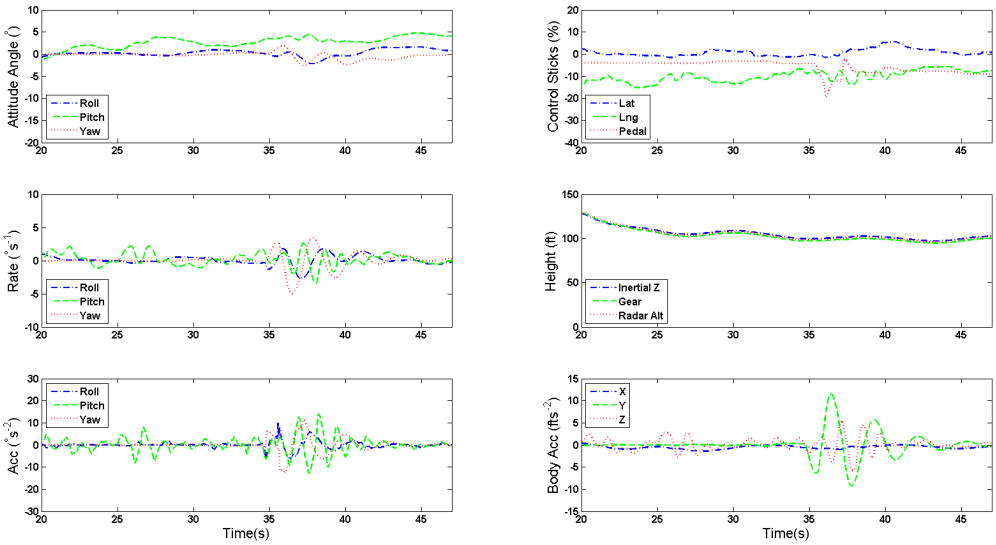

Figure 15: Dynamic responses of GA aircraft and pilot's controls during wake encounter, WTN250 wind turbine hub height 100 ft, wind speed 10 m/s, crossing encounter, offset 1.5D.